Breaking a Lewis Acidity Trend for Rare Earths by Excited State Quenching

Randall K. Wilharm[1], Michael R. Gau,[2] Dirk Trauner[2]*, Eric J. Schelter[1,3,4]*

[1]Vagelos Laboratory for Energy Science and Technology, Department of Chemistry, University of Pennsylvania, Philadelphia, PA 19104, USA

[2]P. Roy and Diana T. Vagelos Laboratories, Department of Chemistry, University of Pennsylvania, Philadelphia, Pennsylvania 19104, USA

[3]Department of Earth and Environmental Science, University of Pennsylvania, Philadelphia, PA 19104, USA

[4]Department of Chemical and Biomolecular Engineering, University of Pennsylvania, Philadelphia, PA 19104, USA

Supporting Information Placeholder

ABSTRACT: Facilitating different chemistries between the rare earth (RE = La-Lu, Sc, Y) ions is of significant interest for their separations. While the bulk of attention has been on maximizing the small differences in their ground state chemistry, interest is beginning to shift towards the differences in their electronic excited states. In this work, we demonstrate modulation of the photostationary state of an azobenzene derivative, Na**1**, via chelation to a series of RE^{III}DO3A (DO3A = 1,4,7,10-tetraazacyclododecane-1,4,7-triacetic acid) complexes. The extent of photoisomerization of **1**$^{-}$ follows the trend in RE^{III} Lewis acidity with two exceptions: Sm^{III} and Er^{III}. UV-Vis spectroscopy, titration experiments, and computational analysis show these exceptions are a result of energy transfer rather than differences in ground state chemistry. These results open a pathway to differentiate REs by a new photochemical means.

Rare earth (RE) elements: the lanthanides (La-Lu), Sc, and Y, are well-established to exhibit similar chemical properties,[1] while the unique magnetic and photophysical properties of individual RE elements are invaluable in permanent magnets,[2] optics,[3] and luminescent probes.[4] Due to their importance and the challenges associated with individual RE element purification by solvent extraction, the REs have been identified as “critical materials”.[5–7] Individual separation of REs from mixed feedstocks have primarily targeted the small and continuous decrease in ionic radii of the RE^{III} cations, e.g. using coordination chemistry, requiring sequential separation of the ions, with its associated cost of solvents and energy.[8] As such, there is a long-standing, and yet unrealized, interest in developing targeted RE separations based on individual cation properties.[9] Notably, the electronic excited state energies of the RE^{III} cations differ greatly between neighbors, which might offer a means to chemically differentiate the ions.

Differentiation between some RE^{III} ions in photochemical processes are known based on oxidation state changes, including photoinduced reduction of Eu^{III} to Eu^{II},[10–12] and photo-oxidation of Ce^{III} to Ce^{IV}.[13] While promising, the underlying mechanism for these processes rely on redox chemistries of the ions, which are not accessible for other RE^{III} cations under mild conditions. We recently showed that *excited state energy transfer* to Dy^{III} 4f states slows an oxygen atom transfer reaction compared to the nearly identical-sized Y^{III}, which lacks an appropriate energy transfer pathway (Figure 1a).[14] This discovery indicates the potential of targeted RE photo-separations by tuning ligand excited states to match with RE^{III} ions. However, reversibility of the photochemical reactions would be an important attribute to achieve future separations system incorporating light.

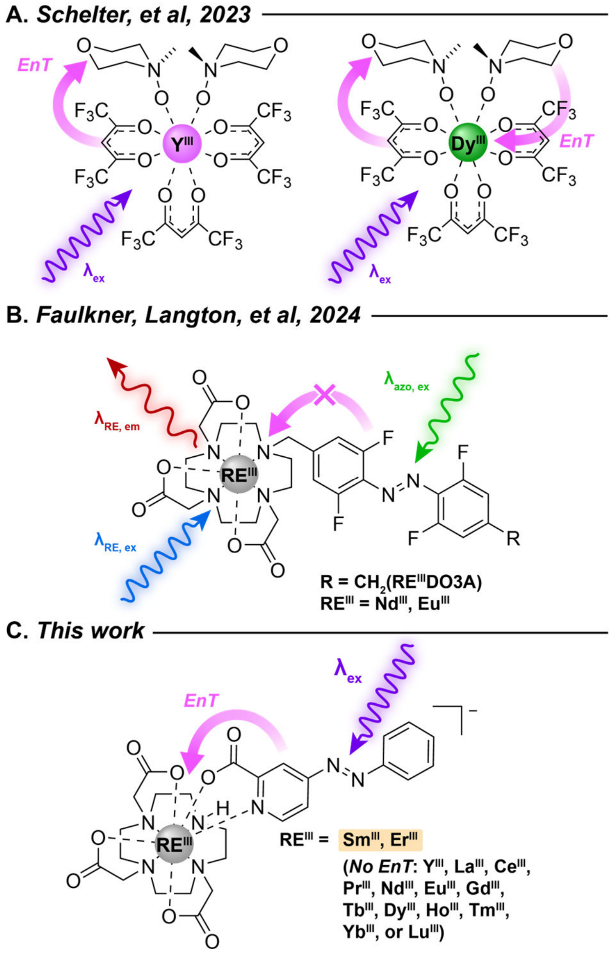

Figure 1. Photochemical studies with RE^{III} complexes showing (a) differentiation of RE^{III} complex reactivity via energy transfer, (b) orthogonality of RE^{III} photoluminescence and ligand photoswitching, and (c) our work in which photoswitching is quenched by energy transfer to select RE^{III} centers.

Photoswitches, such as azobenzenes, have attracted attention for their reversible isomerization, diversity in chemical and photophysical properties, and broad utility.[15] Studies of the effect of proximate RE$^{\mathrm{III}}$ cations on the properties of photoswitches have yielded mixed results. Azobenzene complexes were shown to sensitize the near infrared luminescence of Nd$^{\mathrm{III}}$ and Yb$^{\mathrm{III}}$,[16–18] with limited investigation on the effect of these RE$^{\mathrm{III}}$ ions on photoisomerization. Other photoswitchable ligands (N_2^{2-} and $[C_9H_9]^-$) have shown that modulation of the RE$^{\mathrm{III}}$ metals alter the photoswitch properties of the complexes.[19,20] However, the majority of reported RE$^{\mathrm{III}}$-azobenzene complexes show no modulation of the photoisomerization through interactions with proximate RE$^{\mathrm{III}}$ cations.[21–27] Indeed, Faulkner, Langton, and co-workers recently studied Eu$^{\mathrm{III}}$ and Nd$^{\mathrm{III}}$ complexes with azobenzene-functionalized 1,4,7,10-tetraazacyclododecane-1,4,7-triacetic acid (DO3A) ligands for development of optical memory storage media and concluded that energy transfer to the metal cations was completely absent in the observed photophysical properties of those complexes (Figure 1b).[28]

In this work, we study the photophysical properties of a chelating azobenzene derivative upon coordination to RE$^{\mathrm{III}}$ complexes: [RE$^{\mathrm{III}}$(DO3A)-**1**]$^-$. We demonstrate a Lewis acidity trend in the extent of isomerization at the optimized photostationary state (PSS). Importantly, a break in this trend is observed for RE = Sm or Er, which reach much lower *Z*/*E* ratios at the PSS than would be expected based on Lewis acidity. This is attributed to energy transfer from the excited ligand **1** to Sm$^{\mathrm{III}}$ and Er$^{\mathrm{III}}$ excited states, quenching photoisomerization (Figure 1c). These results are an important finding towards generating single ion-selective reactivity among a series of REs that disrupts typical trends in the chemistry of these metals, towards a new basis for selective RE separations.

Scheme 1. Synthesis of Na1.

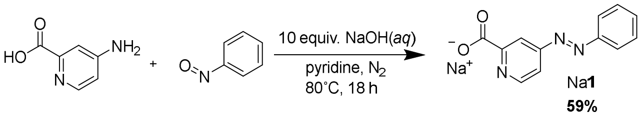

Na**1**
59%

Direct coordination of one of the aryl moieties of an azobenzene is desirable for maximum energy transfer, as the sensitization efficiency of the lanthanides from organic moieties is strongly dependent on the donor-acceptor distance.[29] The picolinate group has been previously established to form stable complexes of RE$^{\mathrm{III}}$ cations[30] and is structurally similar to the 4-pyridyl moiety of azobenzene utilized in other photoswitchable metal complexes.[31,32] For these reasons, the bidentate picolinate azobenzene (Na**1**, Scheme 1) was targeted. The ligand Na**1** was synthesized by Baeyer-Mills coupling and isolated as orange crystals. A scan of irradiation wavelength found 360 nm light to induce the lowest absorbance at 314 nm, indicating a maximized *Z*/*E* ratio (0.05, Figures S1) for Na**1**. To ensure 1:1 coordination of the bidentate azobenzene derivative to a RE$^{\mathrm{III}}$ metal center, the DO3A ligand was chosen (Scheme 2). The RE$^{\mathrm{III}}$-DO3A (RE = Y, La, Ce, Pr, Nd, Sm, Eu, Gd, Tb, Dy, Ho, Er, Tm, Yb, or Lu) complexes were synthesized according to literature procedure with additional HPLC purification to remove all uncoordinated RE$^{\mathrm{III}}$ species (see Supporting Information).[33,34]

The association constants (*K*) of Na**1** to the RE$^{\mathrm{III}}$-DO3A (RE = Y, La, Nd, Sm, Eu, Ho, Er, Tm, Yb, and Lu) complexes in methanol were measured by UV-Vis absorption spectroscopy titration (Figure S2-S4, Table S1).[35,36] Speciation analysis showed that a sizable proportion of **1**$^-$ was not coordinated to the RE$^{\mathrm{III}}$DO3A (as little as 44% coordinated for La$^{\mathrm{III}}$) at a 1:1 stoichiometry at these concentrations ([Na**1**] = 50 μM). Increasing the relative concentration of RE$^{\mathrm{III}}$DO3A to 2 equiv. in relation to Na**1** ensures at least 94% of **1**$^-$ is coordinated for all RE$^{\mathrm{III}}$DO3A except La$^{\mathrm{III}}$ (Table S1, 65%). We next turned to evaluating the photochemistry of the series though PSS determination.

Scanning the irradiation wavelengths for each of the RE$^{\mathrm{III}}$ complexes found 355 nm irradiation to induce the largest change in the UV-Vis absorption spectra. This differs slightly from the free **1**$^-$ due to the change in the spectra upon coordination with a RE$^{\mathrm{III}}$. To investigate the effect each RE$^{\mathrm{III}}$ metal has on the photoisomerization of coordinated **1**$^-$, a solution of 2:1 RE$^{\mathrm{III}}$-DO3A:Na**1** was prepared in methanol and continuously irradiated with 355 nm light while monitoring by UV-Vis absorption spectroscopy from 250 – 600 nm at 25 °C until the PSS was reached (10 – 90 min). Upon irradiation, the absorbance values at 320 nm decreased, characteristic of azobenzene *E* to *Z* photoisomerization (Figure S5-S20). Large differences in the absorbance at the PSS, as well as the rate to reach the PSS, for the RE$^{\mathrm{III}}$ complexes of **1**$^-$ were observed, depending on the identity of the RE$^{\mathrm{III}}$ present (Figure S21). The percentages of the *E* and *Z* isomers present at the PSS of each complex were calculated from UV-Vis absorption spectra using Fischer's method (see Supporting Information)[37] and are shown in Figure S22 and Table S2. The largest, least Lewis acidic RE$^{\mathrm{III}}$ cations, La$^{\mathrm{III}}$ to Pr$^{\mathrm{III}}$, indicated a change in absorbance comparable to that of Na**1** with no RE$^{\mathrm{III}}$-DO3A present. Starting with Nd$^{\mathrm{III}}$, the change in absorbance, and therefore the extent of isomerization, increases with decreasing RE$^{\mathrm{III}}$ cation size to Yb$^{\mathrm{III}}$, which showed the largest change in absorbance from a PSS absorbance value of ~0.9 (0.05 mM) for Na**1** to a PSS absorbance of 0.6.

This trend, with more *Z* isomer present at the PSS with the smaller cations, indicates a Lewis acidity effect. Such trends for the rare earth elements are well-known to produce differences in their chemistries across the series.[38,39] Inflection points in these trends, observed here for Lu$^{\mathrm{III}}$, are also frequently observed, typically attributed to changes in binding modality.[40] For **1**, increasing the Lewis acidity of the coordinating metal, up until Yb$^{\mathrm{III}}$, evidently increases the extent of isomerization at the PSS. The half-lives of the thermal relaxation of Na[RE$^{\mathrm{III}}$DO3A-**1**] correlate more strongly with the %*E* of the sample at the PSS than with the Lewis acidity of the RE$^{\mathrm{III}}$ cation (Figures S23-S24 and Table S3). This result indicates the increased ratio of *Z*/*E* with Lewis acidity cannot be explained by a decrease in the rate of thermal relaxation. The absorbance of [RE$^{\mathrm{III}}$DO3A-(*E*-**1**)] at 355 nm shows little dependence on the identity of RE$^{\mathrm{III}}$ (Figures S6-20), also excluding an increase in absorptivity of the *E* isomer as an explanation for the trend in Lewis acidity. A decrease in the absorbance of [RE$^{\mathrm{III}}$DO3A-(*Z*-**1**)], slowing the reverse photoisomerization process is possible, but absorption spectra of sufficient precision of the *Z* isomer could not be calculated, as yet, to verify this hypothesis.

Scheme 2. Coordination of Na1 to RE$^{\mathrm{III}}$-DO3A and isomerization.

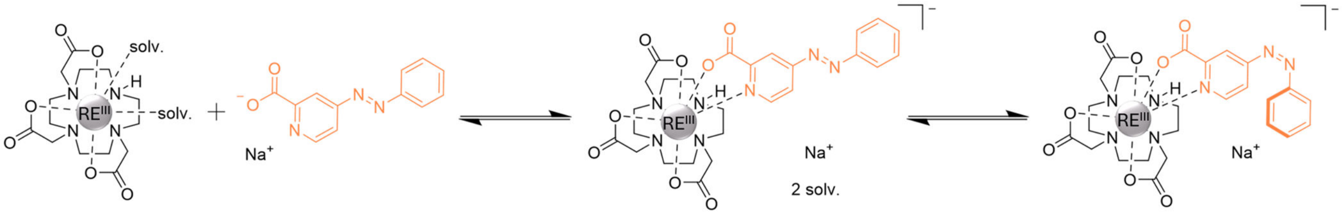

In both the PSS and the thermal relaxation analysis, two RE^{III} complexes show an exception to the Lewis acidity trend: Sm^{III}DO3A and Er^{III}DO3A (Figure 2, green points), which display an anomalously small change in absorbance at the PSS compared to neighboring cations. The PSS absorbance recorded for Na[Er^{III}(DO3A)-**1**] was 0.78, which is larger than the value of 0.67 that might be expected for this complex, while that for Na[Sm^{III}(DO3A)-**1**] was 0.95, compared to an expected value of 0.86 (Figure S25). As such, an additional factor must determine the PSS of those RE = Sm, Er complexes: quenching by their 4f excited states. While azobenzenes have short excited state lifetimes (~10^{-10} - 10^{-12} s)[41] and are thus rarely shown to experience excited state quenching, we propose that Sm^{III} and Er^{III} provides an efficient enough pathway to depopulate the excited state of **1** to compete with photoisomerization (Figure 3).

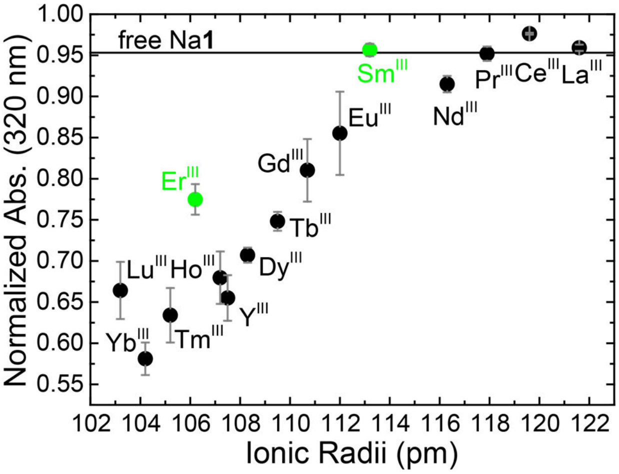

Figure 2. (a) Absorbance at 320 nm of a solution of Na**1** and 2 equivalents of the indicated RE^{III}-DO3A at the PSS irradiated with 355 nm light normalized to the dark adjusted sample (100% *E* isomer). Error bars represent standard deviations (n = 3). Experimental conditions: [Na**1**] = 50 µM, [RE^{III}-DO3A] = 100 µM in methanol, 25 °C.

To further investigate the likely energy transfer pathways between **1** and the paramagnetic RE^{III} cations, we performed DFT calculations to determine the energy levels of the excited states of [Y^{III}(DO3A)-**1**]$^-$. Geometry optimization and conformational search confirmed the global minimum (Figure S26), and excited state calculations were conducted using TD-DFT and ΔSCF (see Supporting Information for details). The $\pi \rightarrow \pi^*$ state (S_6, 28457 cm^{-1}) of **1**, several predicted singlet states between 26000 and 28000 cm^{-1} with low oscillator strength, and the $n \rightarrow \pi^*$ state (S_1, 20008 cm^{-1}) match well with 4f states of Sm^{III} and Er^{III} to allow energy transfer (Figure 3). Photoisomerization of azobenzenes has been shown to primarily proceed through singlet excited states.[41] However, due to the increase in intersystem crossing rates induced by the proximate rare earth cations, involvement of the triplet states of **1**$^-$ cannot be excluded. The two lowest triplet states obtained from TD-DFT (T_2 = 17807 cm^{-1} and T_1 = 14084 cm^{-1}) match favorably with Er^{III}, but are >3600 cm^{-1} higher in energy than the closest downhill Sm^{III} state ($^6F_{11/2}$). The emitting state of Sm^{III} ($^4G_{5/2}$ = 17878 cm^{-1}) is located above these triplet states, indicating population of the emitting state would be rapidly depopulated by energy transfer to these triplet states and thereby quenching Sm^{III} luminescence. Spectroscopic analysis of the luminescence of Na[Sm^{III}DO3A-**1**] found no increase in emission intensity compared to Sm^{III}DO3A with an excitation wavelength of 355 nm, supporting this proposed energy transfer pathway. Further, if the true T_1 energy is closer to that calculated by ΔSCF (8907 cm^{-1}), favorable matches with Sm^{III} and Er^{III} 4f states exist which terminate the energy transfer pathway with metal-based excited states. While a plausible quenching pathway for Sm^{III} and Er^{III} is put forth, many other RE^{III} also have excited states with good energy matching (e.g. Eu^{III} and Ho^{III}, Figure S27). To fully understand the differences in behavior between these RE^{III} complexes, a more detailed modeling of the energy transfer process is needed, as noted previously.[14]

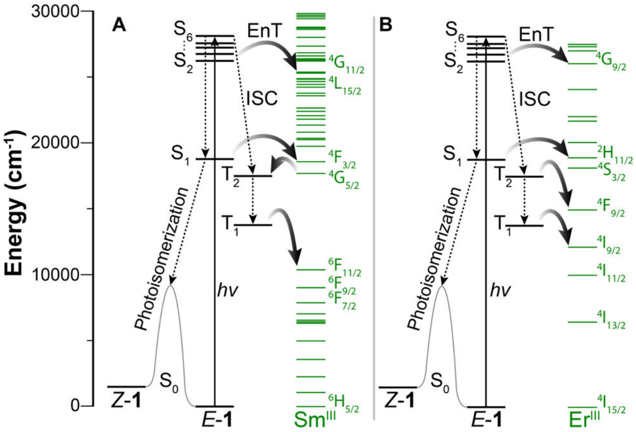

Figure 3. Energy level diagram illustrating the proposed photoisomerization quenching of (a) Sm^{III} and (b) Er^{III} via energy transfer.

We have demonstrated a Lewis acidity trend in the photoisomerization of an azobenzene (**1**$^-$) coordinated to RE^{III}DO3A with two important exceptions: Sm^{III} and Er^{III}. These exceptions cannot be explained by binding strength or ionic radii differences alone. Rather, photoisomerization quenching by energy transfer from **1** to Sm^{III} or Er^{III} as shown in Figure 3 adequately explains this break in the trend. Computational analysis of the excited states of [Y^{III}DO3A-**1**]$^-$ reveal good energy matching between the relevant states of **1** and the known 4f-4f states of Sm^{III} or Er^{III} to facilitate efficient energy transfer. However, due to the known inaccuracies of these computational methods, lack of knowledge of the precise energy levels of the RE^{III} in this system, and lack of observed luminescence, detailed modeling of the energy transfer process is outside the scope of this study and will be investigated subsequently. Regardless, these results reveal a promising avenue for RE^{III} differentiation by incorporation of azobenzene photoswitches and work is currently underway to better understand and exploit the findings of this work.

ASSOCIATED CONTENT

Supporting Information

The Supporting Information is available free of charge on the ACS Publications website.

Spectroscopic data, binding isotherms, binding constants, computed energy level diagram, computational details, synthetic procedures, and crystallographic data for Na**1**. (PDF)

AUTHOR INFORMATION

Corresponding Authors

Eric J. Schelter − Vagelos Laboratory for Energy Science and Technology, Department of Chemistry, University of Pennsylvania, Philadelphia, PA 19104, USA; orcid.org/0000-0002-8143-6206; Email: schelter@sas.upenn.edu

Dirk H. Trauner − P. Roy and Diana T. Vagelos Laboratories, Department of Chemistry, University of Pennsylvania, Philadelphia, Pennsylvnia 19104, USA; orcid.org/0000-0002-6782-6056; Email: dtrauner@upenn.com

Authors

Randall K. Wilharm - Vagelos Laboratory for Energy Science and Technology, Department of Chemistry, University of Pennsylvania, Philadelphia, PA 19104, USA; https://orcid.org/0000-0001-7930-1452

Notes

The authors declare no competing financial interests.

ACKNOWLEDGMENT

The authors thank Dr. Willian W. Brennessel for collection of elemental analysis data. E.J.S. also acknowledges the U.S. Department of Energy, Office of Science, Office of Basic Energy Sciences, Separation Science program under Award DE-SC0017259. E.J.S. and D.T. thank the Vagelos Institute for Energy Science and Technology (VIEST) for support of R.K.W. The authors also thank the University of Pennsylvania for support. This work used Expanse at the San Diego Supercomputing Center[42] through allocation CHE140012 from the Advanced Cyberinfrastructure Coordination Ecosystem: Services & Support (ACCESS) program,[43] which is supported by U.S. National Science Foundation grants #2138259, #2138286, #2138307, #2137603, and #2138296.

REFERENCES

(1) Huang, C.; Bian, Z. Introduction. In *Rare Earth Coordination Chemistry*; John Wiley & Sons, Ltd, 2010; pp 1–39. https://doi.org/10.1002/9780470824870.ch1.

(2) Dent, P. C. Rare Earth Elements and Permanent Magnets (Invited). *J. Appl. Phys.* **2012**, *111* (7), 07A721. https://doi.org/10.1063/1.3676616.

(3) Song, X.; Chang, M.-H.; Pecht, M. Rare-Earth Elements in Lighting and Optical Applications and Their Recycling. *JOM* **2013**, *65* (10), 1276–1282. https://doi.org/10.1007/s11837-013-0737-6.

(4) Cho, U.; Chen, J. K. Lanthanide-Based Optical Probes of Biological Systems. *Cell Chem. Biol.* **2020**, *27* (8), 921–936. https://doi.org/10.1016/j.chembiol.2020.07.009.

(5) *Critical Material Assessment*; U.S. Department of Energy, 2023.

(6) *Recycling of Critical Minerals*; IEA: Paris, 2024. https://www.iea.org/reports/recycling-of-critical-minerals.

(7) Nassar, N. T.; Brainard, J.; Gulley, A.; Manley, R.; Matos, G.; Lederer, G.; Bird, L. R.; Pineault, D.; Alonso, E.; Gambogi, J.; Fortier, S. M. Evaluating the Mineral Commodity Supply Risk of the U.S. Manufacturing Sector. *Sci. Adv.* **2020**, *6* (8), eaay8647. https://doi.org/10.1126/sciadv.aay8647.

(8) Islam, M. F.; Lin, L.; Ray, D.; Premadasa, U. I.; Ma, Y.-Z.; Sacci, R. L.; Kertesz, V.; Custelcean, R.; Bryantsev, V. S.; Doughty, B.; Thiele, N. A. Conformationally Adaptable Extractant Flexes Strong Lanthanide Reverse-Size Selectivity. *J. Am. Chem. Soc.* **2025**, *147* (6), 5080–5088. https://doi.org/10.1021/jacs.4c15074.

(9) Ferguson, A. J.; Gish, M. K. Potential for Light-Induced Separation of Critical Rare-Earth Elements. *Trends in Chemistry* **2024**, *6* (8), 432–446. https://doi.org/10.1016/j.trechm.2024.06.006.

(10) Hirai, T.; Komasawa, I. Separation of Eu from Sm/Eu/Gd Mixture by Photoreductive Stripping in Solvent Extraction. *Ind. Eng. Chem. Res.* **1995**, *34* (1), 237–243. https://doi.org/10.1021/ie00040a024.

(11) de Morais, C. A.; Ciminelli, V. S. T. Europium Recovery by Photochemical Reduction from Eu and Eu–Gd Chloride Solutions. *Sep. Sci. Technol.* **2002**, *37* (14), 3305–3321. https://doi.org/10.1081/SS-120006163.

(12) Bogaert, B. V. den; Havaux, D.; Binnemans, K.; Gerven, T. V. Photochemical Recycling of Europium from Eu/Y Mixtures in Red Lamp Phosphor Waste Streams. *Green Chem.* **2015**, *17* (4), 2180–2187. https://doi.org/10.1039/C4GC02140A.

(13) Livshits, M. Y.; Wolford, N. J.; Banh, J. K.; MacInnes, M. M.; Greer, S. M.; Vellore Winfred, J. S. R.; Hanson, K.; Gompa, T. P.; Stein, B. W. Exploring Differences in Lanthanide Excited State Reactivity Using a Simple Example: The Photophysics of La and Ce Thenoyltrifluoroacetone Complexes. *Inorg. Chem.* **2023**, *62* (34), 13712–13721. https://doi.org/10.1021/acs.inorgchem.3c00717.

(14) Ruoff, K. P.; Gish, M. K.; Song, E.; Douair, I.; Pandey, P.; Steger, M.; Johnson, J. C.; Carroll, P. J.; Gau, M.; Chang, C. H.; Larsen, R. E.; Ferguson, A. J.; Schelter, E. J. Mediating Photochemical Reaction Rates at Lewis Acidic Rare Earths by Selective Energy Loss to 4f-Electron States. *J. Am. Chem. Soc.* **2023**, *145* (30), 16374–16382. https://doi.org/10.1021/jacs.3c01675.

(15) *Molecular Switches*, 2nd ed.; Feringa, B. L., Browne, W. R., Eds.; Wiley, 2011. https://doi.org/10.1002/9783527634408.

(16) Placidi, M. P.; Villaraza, A. J. L.; Natrajan, L. S.; Sykes, D.; Kenwright, A. M.; Faulkner, S. Synthesis and Spectroscopic Studies on Azo-Dye Derivatives of Polymetallic Lanthanide Complexes: Using Diazotization to Link Metal Complexes Together. *J. Am. Chem. Soc.* **2009**, *131* (29), 9916–9917. https://doi.org/10.1021/ja904362f.

(17) Aita, K.; Temma, T.; Kuge, Y.; Seki, K.; Saji, H. NIR Fluorescent Ytterbium Compound for in Vivo Fluorescence Molecular Imaging. *Luminescence* **2010**, *25* (1), 19–24. https://doi.org/10.1002/bio.1136.

(18) Cieslikiewicz-Bouet, M.; V. Eliseeva, S.; Aucagne, V.; F. Delmas, A.; Gillaizeau, I.; Petoud, S. Near-Infrared Emitting Lanthanide(Iii) Complexes as Prototypes of Optical Imaging Agents with Peptide Targeting Ability: A Methodological Approach. *RSC Adv.* **2019**, *9* (3), 1747–1751. https://doi.org/10.1039/C8RA09419E.

(19) Yuan, M.; McNeece, A. J.; Dolgopolova, E. A.; Wolfsberg, L.; Bowes, E. G.; Batista, E. R.; Yang, P.; Filatov, A.; Davis, B. L. Photoinduced Isomerization of [N2]2– in a Bimetallic Lutetium Complex. *J. Am. Chem. Soc.* **2024**, *146* (45), 31074–31084. https://doi.org/10.1021/jacs.4c10950.

(20) Pedussaut, L.; Mahieu, N.; Chartier, C.; Rajeshkumar, T.; Tricoire, M.; Douair, I.; Casaretto, N.; Maron, L.; Danoun, G.; Nocton, G. The Photo-Isomerization of the Cyclononatetraenyl Ligand and Related Rare Earth Complexes. *Chem. Sci.* **2024**, *15* (46), 19273–19282. https://doi.org/10.1039/D4SC04767B.

(21) Lin, L.-R.; Wang, X.; Wei, G.-N.; Tang, H.-H.; Zhang, H.; Ma, L.-H. Azobenzene-Derived Tris-β-Diketonate Lanthanide Complexes: Reversible Trans-to-Cis Photoisomerization in Solution and Solid State. *Dalton Trans.* **2016**, *45* (38), 14954–14964. https://doi.org/10.1039/C6DT01310D.

(22) Lin, L. R.; Tang, H. H.; Wang, Y. G.; Wang, X.; Fang, X. M.; Ma, L. H. Functionalized Lanthanide(III) Complexes Constructed from Azobenzene Derivative and β-Diketone Ligands: Luminescent, Magnetic, and Reversible Trans-to-Cis Photoisomerization Properties. *Inorg. Chem.* **2017**, *56* (7), 3889–3900. https://doi.org/10.1021/acs.inorgchem.6b02819.

(23) Wang, Y.-G.; Li, Y.-Q.; Tang, H.-H.; Lin, L.-R.; Ma, L.-H. Near-Infrared Photoluminescence and Reversible Trans-to-Cis Photoisomerization of Mononuclear and Binuclear Ytterbium(III) Complexes Functionalized by Azobenzene Groups. *ACS Omega* **2018**, *3* (5), 5480–5490. https://doi.org/10.1021/acsomega.8b00386.

(24) Fu, C.-Y.; Chen, L.; Wang, X.; Lin, L.-R. Synthesis of Bis-β-Diketonate Lanthanide Complexes with an Azobenzene Bridge and Studies of Their Reversible Photo/Thermal Isomerization Properties. *ACS Omega* **2019**, *4* (13), 15530–15538. https://doi.org/10.1021/acsomega.9b01817.

(25) Yu, H.-J.; Wang, H.; Shen, F.-F.; Li, F.-Q.; Zhang, Y.-M.; Xu, X.; Liu, Y. Cyclodextrin-Confined Supramolecular Lanthanide Photoswitch. *Small* **2022**, *18* (24), 2201737. https://doi.org/10.1002/smll.202201737.

(26) Guesdon-Vennerie, A.; Couvreur, P.; Ali, F.; Pouzoulet, F.; Roulin, C.; Martínez-Rovira, I.; Bernadat, G.; Legrand, F.-X.; Bourgaux, C.; Mazars, C. L.; Marco, S.; Trépout, S.; Mura, S.; Mériaux, S.; Bort, G. Breaking Photoswitch Activation Depth Limit Using Ionising Radiation Stimuli Adapted to Clinical Application. *Nat. Commun.* **2022**, *13* (1), 4102. https://doi.org/10.1038/s41467-022-30917-0.

(27) Qian, C.; Ma, Y.; Zhang, Y.; Yuan, L.; Zhang, D.; Zhao, L.; Luo, J.; Wang, X. A Multi-Input/Multi-Output Molecular System Based on Lanthanide(III) Complexes. *Inorg. Chem. Front.* **2022**, *9* (11), 2668–2675. https://doi.org/10.1039/D2QI00360K.

(28) Simms, C. H.; Nielsen, V. R. M.; Sørensen, T. J.; Faulkner, S.; Langton, M. J. Photoswitchable Luminescent Lanthanide Complexes Controlled and Interrogated by Four Orthogonal

Wavelengths of Light. *Phys. Chem. Chem. Phys.* **2024**, *26* (27), 18683–18691. https://doi.org/10.1039/D4CP02243B.

(29) Bünzli, J.-C. G. On the Design of Highly Luminescent Lanthanide Complexes. *Coord. Chem. Rev.* **2015**, *293–294*, 19–47. https://doi.org/10.1016/j.ccr.2014.10.013.

(30) Powell, J. E.; Ingemanson, J. W. Lanthanide Picolinate Chelate Stabilities. *Inorg. Chem.* **1968**, *7* (11), 2459–2461. https://doi.org/10.1021/ic50069a058.

(31) Telleria, A.; van Leeuwen, P. W. N. M.; Freixa, Z. Azobenzene-Based Ruthenium(II) Catalysts for Light-Controlled Hydrogen Generation. *Dalton Trans.* **2017**, *46* (11), 3569–3578. https://doi.org/10.1039/C7DT00542C.

(32) Gong, D.; Kong, D.; Xu, N.; Hua, Y.; Liu, B.; Xu, Z. Bidentate Ru(II)-NC Complex as a Catalyst for Semihydrogenation of Azoarenes to Hydrazoarenes with Ethanol. *Org. Lett.* **2022**, *24* (40), 7339–7343. https://doi.org/10.1021/acs.orglett.2c02866.

(33) Dischino, D. D.; Delaney, E. J.; Emswiler, J. E.; Gaughan, G. T.; Prasad, J. S.; Srivastava, S. K.; Tweedle, M. F. Synthesis of Nonionic Gadolinium Chelates Useful as Contrast Agents for Magnetic Resonance Imaging: 1,4,7-Tris(Carboxymethyl)-10-Substituted-1,4,7,10-Tetraazacyclododecanes and Their Corresponding Gadolinium Chelates. *Inorg. Chem.* **1991**, *30* (6), 1265–1269. https://doi.org/10.1021/ic00006a020.

(34) Jagadish, B.; Brickert-Albrecht, G. L.; Nichol, G. S.; Mash, E. A.; Raghunand, N. On the Synthesis of 1,4,7-Tris(Tert-Butoxycarbonylmethyl)-1,4,7,10-Tetraazacyclododecane. *Tetrahedron Lett.* **2011**, *52* (17), 2058–2061. https://doi.org/10.1016/j.tetlet.2010.10.074.

(35) Http://Supramolecular.Org/.

(36) Brynn Hibbert, D.; Thordarson, P. The Death of the Job Plot, Transparency, Open Science and Online Tools, Uncertainty Estimation Methods and Other Developments in Supramolecular Chemistry Data Analysis. *Chem. Commun.* **2016**, *52* (87), 12792–12805. https://doi.org/10.1039/c6cc03888c.

(37) Fischer, E. Calculation of Photostationary States in Systems A⇌B When Only A Is Known. *J. Phys. Chem.* **1967**, *71* (11), 3704–3706. https://doi.org/10.1021/j100870a063.

(38) Cacheris, W. P.; Nickle, S. K.; Sherry, A. D. Thermodynamic Study of Lanthanide Complexes of 1,4,7-Triazacyclononane-N,N',N"-Triacetic Acid and 1,4,7,10-Tetraazacyclododecane-N,N',N",N'''-Tetraacetic Acid. *Inorg. Chem.* **1987**, *26* (6), 958–960. https://doi.org/10.1021/ic00253a038.

(39) Cotton, S. A.; Raithby, P. R. Systematics and Surprises in Lanthanide Coordination Chemistry. *Coordination Chemistry Reviews* **2017**, *340*, 220–231. https://doi.org/10.1016/j.ccr.2017.01.011.

(40) Hu, A.; Aluicio-Sarduy, E.; Brown, V.; Macmillan, S. N.; Becker, K. V.; Barnhart, T. E.; Radchenko, V.; Ramogida, C. F.; Engle, J. W.; Wilson, J. J. Py-Macrodipa: A Janus Chelator Capable of Binding Medicinally Relevant Rare-Earth Radiometals of Disparate Sizes. *J. Am. Chem. Soc.* **2021**, *143* (27), 10429–10440. https://doi.org/10.1021/jacs.1c05339.

(41) Lednev, I. K.; Ye, T.-Q.; Hester, R. E.; Moore, J. N. Femtosecond Time-Resolved UV−Visible Absorption Spectroscopy of *Trans*-Azobenzene in Solution. *J. Phys. Chem.* **1996**, *100* (32), 13338–13341. https://doi.org/10.1021/jp9610067.

(42) Strande, S.; Cai, H.; Tatineni, M.; Pfeiffer, W.; Irving, C.; Majumdar, A.; Mishin, D.; Sinkovits, R.; Norman, M.; Wolter, N.; Cooper, T.; Altintas, I.; Kandes, M.; Perez, I.; Shantharam, M.; Thomas, M.; Sivagnanam, S.; Hutton, T. Expanse: Computing without Boundaries: Architecture, Deployment, and Early Operations Experiences of a Supercomputer Designed for the Rapid Evolution in Science and Engineering. In *Practice and Experience in Advanced Research Computing*; ACM: Boston MA USA, 2021; pp 1–4. https://doi.org/10.1145/3437359.3465588.

(43) Boerner, T. J.; Deems, S.; Furlani, T. R.; Knuth, S. L.; Towns, J. ACCESS: Advancing Innovation: NSF's Advanced Cyberinfrastructure Coordination Ecosystem: Services & Support. In *Practice and Experience in Advanced Research Computing*; ACM: Portland OR USA, 2023; pp 173–176. https://doi.org/10.1145/3569951.3597559.

TOC Graphic